land

MDPI

Article

Implementing a New Rubber Plant Functional Type in the Community Land Model (CLM5) Improves Accuracy of Carbon and Water Flux Estimation

Ashehad A. Ali [1,*,†], Yuanchao Fan [2,†], Marife D. Corre [3], Martyna M. Kotowska [4], Evelyn Preuss-Hassler [3], Andi Nur Cahyo [5], Fernando E. Moyano [1], Christian Stiegler [1], Alexander Röll [6], Ana Meijide [7], Alexander Olchev [8], Andre Ringeler [1], Christoph Leuschner [4,9], Rahmi Ariani [1], Tania June [10], Suria Tarigan [11], Holger Kreft [9,12], Dirk Hölscher [6,9], Chonggang Xu [13], Charles D. Koven [14], Katherine Dagon [15], Rosie A. Fisher [15], Edzo Veldkamp [3,9] and Alexander Knohl [1,9]

1 Department of Bioclimatology, University of Göttingen, Bioclimatology, 37077 Göttingen, Germany; fernando.moyano@geo.uni-augsburg.de (F.E.M.); christian.stiegler@biologie.uni-goettingen.de (C.S.); aringel@gwdg.de (A.R.); rariani@uni-goettingen.de (R.A.); aknohl@uni-goettingen.de (A.K.)
2 Center for the Environment, Faculty of Arts and Sciences, Harvard University, Cambridge, MA 02138, USA; ycfan@g.harvard.edu
3 Soil Science of Tropical and Subtropical Ecosystems, University of Göttingen, 37077 Göttingen, Germany; mcorre@gwdg.de (M.D.C.); evelynpreuss@posteo.de (E.P.-H.); eveldka@gwdg.de (E.V.)
4 Department of Plant Ecology and Ecosystems Research, University of Göttingen, 37007 Göttingen, Germany; martyna.kotowska@biologie.uni-goettingen.de (M.M.K.); cleusch@gwdg.de (C.L.)
5 Indonesian Rubber Research Institute, Banyuasin 30953, Indonesia; nurcahyo.andi@yahoo.co.uk
6 Tropical Silviculture and Forest Ecology, University of Göttingen, 37007 Göttingen, Germany; aroell@gwdg.de (A.R.); dhoelsc@gwdg.de (D.H.)
7 Department of Crop Sciences, Division Agronomy, University of Göttingen, 37007 Göttingen, Germany; ana.meijideorive@uni-goettingen.de
8 Department of Meteorology and Climatology, Faculty of Geography, Lomonosov Moscow State University, 1199991 Moscow, Russia; aoltche@gmail.com
9 Centre of Biodiversity and Sustainable Land Use, University of Göttingen, 37007 Göttingen, Germany; holger.kreft@forst.uni-goettingen.de
10 Department of Geophysics and Meteorology, Bogor Agricultural University, Bogor 16680, Indonesia; taniajune@apps.ipb.ac.id
11 Department of Soil and Natural Resources Management, Bogor Agricultural University, Bogor 16680, Indonesia; sdtarigan@apps.ipb.ac.id
12 Biodiversity, Macroecology & Biogeography, University of Göttingen, 37007 Göttingen, Germany
13 Los Alamos National Laboratory, Earth and Environmental Sciences Division, Los Alamos, NM 87545, USA; cxu@lanl.gov
14 Lawrence Berkeley National Laboratory, Climate and Ecosystem Sciences Division, Berkeley, CA 94701, USA; cdkoven@lbl.gov
15 Climate and Global Dynamics Laboratory, National Center for Atmospheric Research, Boulder, CO 80301, USA; kdagon@ucar.edu (K.D.); rosie.fisher@cicero.oslo.no (R.A.F.)
* Correspondence: ashehad.ali@uni-goettingen.de
† These authors contributed equally to this work.

Abstract: Rubber plantations are an economically viable land-use type that occupies large swathes of land in Southeast Asia that have undergone conversion from native forest to intensive plantation forestry. Such land-use change has a strong impact on carbon, energy, and water fluxes in ecosystems, and uncertainties exist in the modeling of future land-use change impacts on these fluxes due to the scarcity of measured data and poor representation of key biogeochemical processes. In this current modeling effort, we utilized the Community Land Model Version 5 (CLM5) to simulate a rubber plant functional type (PFT) by comparing the baseline parameter values of tropical evergreen PFT and tropical deciduous PFT with a newly developed rubber PFT (focused on the parameterization and modification of phenology and allocation processes) based on site-level observations of a rubber clone in Indonesia. We found that the baseline tropical evergreen and baseline tropical deciduous functions and parameterizations in CLM5 poorly simulate the leaf area index, carbon dynamics, and

Citation: Ali, A.A.; Fan, Y.; Corre, M.D.; Kotowska, M.M.; Preuss-Hassler, E.; Cahyo, A.N.; Moyano, F.E.; Stiegler, C.; Röll, A.; Meijide, A.; et al. Implementing a New Rubber Plant Functional Type in the Community Land Model (CLM5) Improves Accuracy of Carbon and Water Flux Estimation. *Land* **2022**, *11*, 183. https://doi.org/10.3390/land11020183

Academic Editor: Nir Krakauer

Received: 13 December 2021
Accepted: 19 January 2022
Published: 24 January 2022

water fluxes of rubber plantations. The newly developed rubber PFT and parametrizations (CLM-rubber) showed that daylength could be used as a universal trigger for defoliation and refoliation of rubber plantations. CLM-rubber was able to predict seasonal patterns of latex yield reasonably well, despite highly variable tapping periods across Southeast Asia. Further, model comparisons indicated that CLM-rubber can simulate carbon and energy fluxes similar to the existing rubber model simulations available in the literature. Our modeling results indicate that CLM-rubber can be applied in Southeast Asia to examine variations in carbon and water fluxes for rubber plantations and assess how rubber-related land-use changes in the tropics feedback to climate through carbon and water cycling.

Keywords: rubber trees; intraspecies differences; carbon–water cycling; CLM; earth system model; land-use change

1. Introduction

The widespread conversion of natural forests into woody plantation crops in tropical regions can strongly impact regional carbon budgets and water resources [1–3]. In Southeast Asia, one of the major drivers of such land-use change has been the demand for rubber [4,5]. Consequently, this land-use type occupies relatively large territories in Southeast Asia and the world. Although rubber trees have been cultivated for several decades [6,7], little is known about how monocultures of these trees differ from natural forests in terms of exchange of carbon dioxide and water vapor with the atmosphere. There exists limited observational data on leaf-level physiology (e.g., photosynthetic capacity, stomatal conductance) [8,9] ecosystem-scale exchanges of gases, water, and energy in rubber plantations [10,11]. Consequently, the temporal and regional variability of such properties for these ecosystems remains unknown.

Understanding carbon and water cycling processes at the site level is the first step in determining how rubber plantations' expansion impacts carbon sequestration, ecosystem services, and other environmental variables. While data from site-level studies that utilize field-based techniques are essential for examining how carbon and water cycling processes are influenced by land-use conversion to rubber plantations [12,13], there are inherent shortcomings when extrapolating short-term site-level observations to longer temporal and larger spatial scales. Therefore, ecosystem modeling that represents a mechanistic understanding of ecosystem function and processes is often used [14]. For example, Kumagai et al. [15] developed a soil–vegetation–atmosphere transfer model for rubber plantations (SVAT-rubber). They examined how canopy structure in the model affected carbon and water fluxes in central Cambodia, while Yang et al. [16] used the Land Use Change Impact Assessment model to simulate rubber (LUCIA) and investigated how high altitudes and planting densities influenced the modeled biomass and latex yield of rubber plantations. It is worth noting that the former study considered only one site, and therefore their results could be site-specific. In contrast, the latter study did not properly simulate rubber's canopy development.

Some statistical models have been developed to predict suitable areas for growing rubber plantations [17–19]. For example, Liu et al. [17] investigated the impacts of future climate change on the suitability of rubber plantations in China by utilizing five main climatic factors. Their results showed that the rubber plantation would have a trend of expansion to the north in 2041–2080. Ray et al. [19] used an ecological niche model to analyze the present and potential future distribution of rubber trees in two biogeographically distinct regions of India, i.e., the Western Ghats (WG) and Northeast (NE). Ray et al. [19] found more areas would be suitable for rubber tree plantation in the NE region, whereas further expansion would be limited in the WG region under the projected climate scenario for 2050. Using a statistical regression model (SRM), Lang et al. [20] disentangled the links between soil water content, soil texture, and mineral nitrogen in rubber plantations and

assessed the impacts of land-use change on methane flux. Land surface models are also increasingly adopted to investigate the impact of land-use change on carbon and energy fluxes at various temporal and spatial scales [21–23]. To simulate vegetation dynamics and interactions with the soil and atmosphere, land surface models usually reduce intra- and interspecies vegetation diversity into a few plant functional types (PFTs), defined by the key physiological and morphological characteristics of specific plant groups and their essential ecological functions [24]. There are several advantages in using a land surface model to investigate terrestrial ecosystem processes and the impact of land-use change, including: (1) an examination of diurnal, seasonal, and longer-term changes in carbon, water, and energy cycling across spatial scales [25,26]; (2) the identification of crucial and sensitive model parameters [26,27]; and (3) assessing historical and future climate change impacts on natural and agroecosystem functioning [23,28].

Phenology is an important aspect of any PFT in land surface models, for it regulates the timing of leaf onset and offset [29,30], the rate of leaf litterfall [31], and associated stomata-level processes of water and carbon exchanges in response to varying environmental conditions. The phenology of rubber varies across regions, making its parameterization challenging in models applied to the global scale. The rubber tree (*Hevea brasiliensis*) is native to the Amazon rainforest [32] but cultivated throughout the tropics. Although native rubber is evergreen, it can turn to semideciduous (facultative deciduous) in other tropical [33] and subtropical environments [7,10]. In locations with a pronounced dry season, the leaf fall period is short, and refoliation occurs before the start of the rainy season [34]. Sustained period of reduced daylength could also trigger leaves to fall in rubber plantations [35,36]. Moreover, the leaf phenology of rubber is associated with reproduction. Empirical data show rubber trees increase their leaf litterfall rates when they allocate carbon to produce fruits [37]. This study introduces and simulates rubber utilizing an advanced land surface model, the Community Land Model version 5 [26,38]. CLM5 currently includes fourteen natural vegetation and eight crop PFTs, which allow an adequate description of the main variety of global vegetation phenology (e.g., evergreen, stress–deciduous, seasonal–deciduous, and annual single-season crops), morphology (e.g., needle-leaf and broadleaf trees, shrubs, and grasses) and physiology (C3 and C4 photosynthesis, carbon and nitrogen allocation, etc.) across different climate zones [39]. However, perennial tree crops are not yet included, even though they occupy an increasing land surface in tropical regions [4]. This is partly because of the limited data available for the parameterization of critical processes. The development of rubber as a PFT in CLM5 will help investigate how the rubber plantations respond to nitrogen fertilization rates and extreme climate events (e.g., those caused by El Nino–Southern Oscillation). Rubber PFT in CLM5 can also simulate the spatial distribution of carbon and water fluxes at regional and continental scales. Since rubber is a facultative deciduous species; that is, it is a partial deciduous species which is evergreen most of the year; it is useful to simulate rubber using baseline values of tropical evergreen PFT or tropical deciduous PFT and compare the model outputs with our newly developed rubber PFT with reference to empirical field measurements of rubber productivity and ecosystem functions.

The main objective of this current modeling effort is to develop a new rubber PFT in CLM5 (and introduce rubber-specific functions) using data from a rubber clone in Jambi, Indonesia. We synthesized the data collected in several short-term field surveys and an intensive one-year measurement campaign in smallholder rubber plantations in Jambi, Indonesia, and subsequently used these data for model calibration. We also compared our modeling results with data from previous rubber modeling studies.

2. Methods

2.1. Study Sites

The main study site used in this research is located in the lowlands of Jambi province, Sumatera, Indonesia (2° S, 103° E, 40–70 m above sea level), with site selection reflecting the fact that a relatively large part of the lowlands in Jambi province was converted to oil

palm and rubber plantations in the previous two decades [6,40]. The region's climate is tropical maritime [41], with mean annual temperature and mean annual precipitation in Jambi averaging 26.7 ± 1.0 °C and 2235 ± 385 mm, respectively [6]. The dry season usually starts in May (~130 mm per month) and lasts until September (~20 mm per month), while the rainy season is between October and April.

Measurements were performed in the Harapan landscape within the Jambi province, characterized by loam Acrisol soils [12], and sites are located about 80 km southwest of Jambi City. Within the landscape, four rubber plantations were chosen and within each plantation, a 50 m × 50 m plot was established [42]. We collated the following measured datasets from each of the four plots: total net primary productivity (*NPP*), leaf litterfall, latex yield, fine root biomass within top 30 cm depth, soil moisture at 5 cm depth, leaf area index (LAI), and transpiration rate. All of the data were obtained between 2012 and 2014, except for the leaf area index, which was measured at the beginning of the dry season in 2018. All of these measured data are cited in the figure captions. Additional information on vegetation characteristics such as rubber tree density, tree height, and basal area can be found in Table 2 of Kotowska et al. [42]. To expand the dataset used for model validation and evaluation beyond the focus area of Jambi province, we additionally extracted available data containing carbon and water-related variables in rubber plantations using following terms: "rubber plantations", "tropics", "rubber trees", "subtropics", "net ecosystem exchange", "leaf area index", "transpiration", "evapotranspiration", "specific leaf area", and "rubber tree growth" from the free web search engines Google Scholar and Web of Science. Selection criteria for data inclusion were matured rubber plantations and field grown rubber trees. A spatial display of all sites used in this study is shown in Figure A1. We were able to obtain six articles corresponding to up to five different rubber plantation sites. These plantation sites were located in Indonesia, Cambodia, Thailand and China.

2.2. Model Initialization

Similar to many land surface models [43], CLM needs to be spun up to bring all soil and vegetation carbon and nitrogen pools into equilibrium [31]. Therefore, to estimate the vegetation and soil biogeochemical state before the establishment of the rubber plantation in Jambi, the model was first spun up to a preindustrial equilibrium state with a Tropical Evergreen forest PFT and continued with a 20th century transient run until 2001, using the standard procedures of CLM spin-ups [44,45]. The Tropical Evergreen PFT for the spin-up was used because it was the region's dominant natural vegetation before the agricultural-driven land-use change. For spin-ups, we used site-level measurements of soil texture [12], the preindustrial value of CO_2 concentration (284.7 ppm), and recycled the climate data of 1900–1972, extracted for the Jambi lowland from CRUNCEP data [46] for the duration of the simulations. CRUNCEP uses two types of data: one that is derived using the NCEP reanalysis at a 6 h time step and 2.5 resolution based on a climate model (that only assimilates the temperatures) and the other the monthly Climate Research Unit (CRU TS Version 4.04) climatology at 0.5 resolution.

We performed the first spin-up by running the model for 300 years in the accelerated mode, whereby the decomposition of slower cycling carbon and nitrogen pools is increased for the duration of the spin-up, and the pool sizes are modified accordingly at the end of the spin-up [28,31]. Then we ran the model for another 300 years in the normal mode to get to the ecosystem equilibrium state. We performed a transient simulation following spin-ups, where we used the CRUNCEP climate data [46] and transient CO_2 across years. Since historical data on CO_2 concentration and N deposition were available from 1850, the transient simulations were performed from 1850 until 2000.

Following the spin-up and 20th century simulations, a clear-cut site disturbance was implemented in the year 2001 by setting the aboveground carbon and nitrogen pools to zero. To this end, we transferred the fine root and coarse root carbon and nitrogen into the litter pools. Then a rubber plantation simulation in Jambi was performed from 2001 to

2014 using the site-level half-hourly climate data [47]. We simulated two separate rubber PFT simulations: (1) one that used baseline parameter values of tropical evergreen PFT and its corresponding functions (hereafter referred to as "AS_EVG") and (2) the other that used baseline parameter values of tropical deciduous PFT and its corresponding functions (hereafter referred to as "AS_DEC").

To evaluate rubber PFT simulations at other sites (those that differ in climate and soil texture from Jambi), we first obtained data from three different sites: SRC, Indonesia (4° S, 104° E; 10 m elevation); CRRI, Cambodia (11.6° N, 105° E; 57 m elevation); and Som Sanuk, Thailand (18.1° N, 103° E; 210 m elevation), and then we performed separate simulations at each site for the "AS_EVG" and "AS_DEC" types using each PFT's baseline parameter values and their corresponding functions. To carry out these rubber PFT simulations at these additional sites, a similar protocol was used as in the case of Jambi, Indonesia. That is, we used their site-specific soil texture and CRUNCEP climate data [46] to perform spin-ups and transient simulations from the year 1850 up to the year before the clear-cut site disturbance was implemented. At that time point, a clear-cut disturbance at every site was carried out by setting the aboveground carbon and nitrogen pools to zero. As in the case of Jambi, we transferred the fine root carbon and nitrogen into fast litter pools at every site. Next, a rubber plantation simulation was performed at each site from their clear-cut year to year 2014 using the site-level half-hourly climate data. The source of the local climate data follows: the data from SRC were directly available to the authors; for the CRRI and Som Sanuk sites, the data were adapted from the repository specified in Giambelluca et al. [10].

2.3. Rubber PFT Development

For the development of the rubber PFT within CLM5, our main goal was to represent the growth characteristics of rubber trees and include a realistic representation of carbon exports via latex harvest. We modified the phenology and allocation schemes of the existing broadleaf tropical deciduous tree PFT to represent rubber's specific leaf onset, litterfall, and harvest export of latex yield that influence carbon and water cycles.

We parameterized and calibrated the model at the Jambi site only. Some parameter values were prescribed using measurement data from Jambi, while other parameter values were obtained via model calibration, e.g., we used measured values of leaf morphological parameters such as the ratio of leaf C to leaf N (leaf CN) and specific leaf area (SLA). For model calibration, we used the specific dataset from Jambi and compared it with Jambi's model output values. Specifically, these measured Jambi data were leaf litterfall rates, transpiration rates, leaf area index, net primary productivity, latex harvest yield, and fine root biomass. We can consider the final set of parameters (measured and calibrated) for the Jambi model simulation as "optimum parameter set values". A list of parameters for CLM5 is provided in Table 1, which shows the default value, measured or calibrated value, and the most affected model output the parameter value impacts (the model is fitted to the corresponding observed values).

2.4. Phenology

We implemented the rubber phenology based on the standard stress deciduous phenology scheme for tropical broadleaf PFT in CLM5 [31]. We first describe the standard stress deciduous phenology scheme (see Appendices B and C) and then describe our changes in this rubber scheme (see below). The standard stress deciduous phenology scheme in CLM5 [31] is based on Dahlin et al. [30] that allows plants to shed their leaves through two different mechanisms: (i) leaf onset/offset—where this switch is triggered by sustained periods of wet or dry soil (Appendix B); (ii) a background leaf litterfall rate, which is calculated using leaf longevity (Appendix C). The background leaf litterfall rate is not associated with a specific offset period but occurs over an extended time.

Table 1. Parameter values for tropical deciduous PFT (default/baseline values) and rubber PFT. The parameterized values are either the measured values taken from literature [14,16,34,41,48,49] or calibrated value.

Parameter	Definition	Unit	Default/ Baseline Value	Rubber Parameter Value	Parameter Type	Modeled Outcomes the Parameter Value Impacts
SWPc	Critical soil water potential (SWP)	MPa	−0.8	−2 or −0.8	calibrated value	- Phenology, leaf offset - Leaf litterfall rates
rho	Factor that multiplies the rate coefficient for background litterfall	unitless	1	1.5	calibrated value	- Phenology, leaf offset - Leaf litterfall rates
f_{tap}	Proportion of latex tapping for wood allocation partitioning	unitless	–	0.46	calibrated value	- C and N allocation - Net primary productivity, yield
SLA	Specific leaf area	$m^2\ g^{-1}C$	0.0308	0.026	measured value from literature	- Net primary productivity - Yield
Leaf longevity	Life of leaf	years	0.483	1	calibrated value	- Net primary productivity - Yield
Stem: leaf	Ratio of stem C to leaf C	unitless	2.3	1	calibrated value	- C and N allocation - Net primary productivity, leaf and stem biomass
leafcn	Leaf C: N	$g\ C\ g^{-1}\ N$	23.45	14.7	measured value from literature	- C and N allocation - Net primary productivity

Table 1. *Cont.*

Parameter	Definition	Unit	Default/ Baseline Value	Rubber Parameter Value	Parameter Type	Modeled Outcomes the Parameter Value Impacts
leafcn_max	Maximum leaf CN ratio	g C g^{-1} N	35	25.3	measured value from literature	- C and N allocation - Net primary productivity
leafcn_min	Minimum leaf CN ratio	g C g^{-1} N	15	10.5	measured value from literature	- C and N allocation - Net primary productivity
dsladlai	Change is specific leaf area per unit change in leaf are index	m^2 g^{-1} C	0.0027	0.0012	calibrated value	- Leaf area index - Net primary productivity
medlynslope	Medlyn slope of conductance–photosynthesis relationship	µmol H_2O $µmol^{-1}$ CO_2	4.45	3.56	calibrated value	- Transpiration - Photosynthesis

2.5. Phenology Scheme for Rubber

The changes we have made in the standard stress deciduous phenology scheme for rubber are based on the following observations. Foremost, we set the leaf longevity (γ_{leaf}) of rubber trees to one year because rubber trees exhibit annual shedding of senescent leaves [50].

Secondly, the defoliation (leaf offset), also referred to as "wintering", is usually seen in rubber trees once they are matured, that is, once they are greater than 4 years old [50–52]. In the Northern Hemisphere, specifically in mainland Asia (e.g., Cambodia and Thailand), rubber plantations have been observed to be in dormancy (LAI = 0) for about three weeks in January [11]. The mechanisms for this dormancy are mixed: reduced soil moisture [11,53] or low temperatures when soil moisture had already recovered [7,54]. In the Southern Hemisphere, dormancy in rubber plantations has been observed in August [55,56]. If the soil is relatively wet and temperatures are relatively high throughout the year, then it is challenging for the model to predict leaf offset (i.e., "predict dormancy") as observed empirically. Our preliminary modeling analyses indicated that all of the aforementioned triggers were unable to predict the leaf offset as empirically observed. Since Yeang et al. [36] and Zhai et al. [37] suggested that decreases in daylength could also trigger leaves to fall in rubber plantations, we used daylength to trigger leaf offset. Below we present a set of four rules for the initiation of leaf offset for varying daylength (hours) values:

$$\text{leaf}_{\text{offset}} = \begin{cases} D_{max} < 12.5 \text{ and } d_{current} \geq D_{min} + 0.011 \text{ and } d_{current} \leq D_{min} + 0.04 \text{ and } d_{current} \geq d_{previous} \\ 12.5 \leq D_{max} < 12.8 \text{ and } d_{current} \geq D_{min} + 0.25 \text{ and } d_{current} \geq d_{previous} \\ 12.8 \leq D_{max} < 13.2 \text{ and } d_{current} \geq D_{min} + 0.38 \text{ and } d_{current} \geq d_{previous} \\ D_{max} \geq 13.2 \text{ and } d_{current} \geq D_{min} + 0.38 \text{ and } d_{current} \leq D_{min} + 0.74 \text{ and } d_{current} \geq d_{previous} \end{cases} \quad (1)$$

where D_{max}, D_{min} is the maximum and minimum values of daylength at a given location, respectively, and $d_{current}$ and $d_{previous}$ are the current and previous day's daylength value at a given location, respectively. The four rules in Equation (1) are evaluated by the logic "OR" and the values in Equation (1) are based on manual calibration. As noted above, we segregated daylength values and also constrain them so that they can be applicable at different sites in Southeast Asia. If the leaves were not in the offset period, then they were in the onset period.

Next, we increased r_{bglf} by multiplying it by 1.5 during the period when the leaf offset was initiated. The value of 1.5 was obtained by fitting the modeled leaf litterfall rates in Jambi to measured leaf litterfall rates in Jambi [34].

Finally, to avoid much longer periods of modeled leaf offset than observed, we modified the value of offset soil water potential threshold as follows:

$$\varphi_{\text{threshold}} = \begin{cases} -2 \text{ for } \text{rain}_{10} = 0 \text{ and } \text{rain}_{60} \leq 30 \\ -0.8 \end{cases}, \quad (2)$$

where rain_{10} is the previous 10 days of accumulated rainfall and rain_{60} is the previous 60 days of accumulated rainfall.

2.6. Allocation Scheme for Latex Harvest Yield

As in the case of phenology, we describe the standard carbon allocation scheme used in CLM5 (see Appendix D). Below we explain our assumptions for rubber to calculate latex harvest yield and also explain how we obtained the parameter value related to tapping. We assume that due to tapping, the total stem allocation would be partitioned to three pools with the following allometry for CLM-rubber,

$$1 = a_4 + f_{tap} + f_d \quad (3)$$

where f_{tap} is the proportion of stem allocation partitioned into latex tapping (f_{tap} = 0.46) and f_d is the allocation for deadwood ($f_d = 1 - a_4 - f_{tap}$). We obtained the value of f_{tap}

by fitting the modeled latex harvest yield of Jambi to the measured latex harvest yield of Jambi. Thus, Equations (A10)–(A13) now change to Equations (4)–(9) as follows;

$$\text{cpool\_to\_livestemc} = \text{CF}_{\text{alloc,leaf\_tot}} * a_3 * a_4 * \text{fcur}, \quad (4)$$

$$\text{cpool\_to\_livestemc\_storage} = \text{CF}_{\text{alloc,leaf\_tot}} * a_3 * a_4 * (1 - \text{fcur}) \quad (5)$$

$$\text{cpool\_to\_deadstemc} = \text{CF}_{\text{alloc,leaf\_tot}} * a_3 * \left(1 - a_4 - f_{\text{tap}}\right) * \text{fcur}, \quad (6)$$

$$\text{cpool\_to\_deadstemc\_storage} = \text{CF}_{\text{alloc,leaf\_tot}} * a_3 * \left(1 - a_4 - f_{\text{tap}}\right) * (1 - \text{fcur}) \quad (7)$$

The carbon flux of the latex harvest yield is calculated as follows,

$$\text{cpool\_to\_tappingc} = \text{CF}_{\text{alloc,leaf\_tot}} * a_3 * f_{\text{tap}} * \text{fcur} \quad (8)$$

$$\text{cpool\_to\_tappingc\_storage} = \text{CF}_{\text{alloc,leaf\_tot}} * a_3 * f_{\text{tap}} * (1 - \text{fcur}) \quad (9)$$

2.7. Tapping Period

We recognized that there was a marked difference between the tapping period for rubber plants located around the equator versus those growing at latitudes greater than 8°. Around the equator, there was no difference in rubber tapping period between the dry and wet seasons (e.g., Jambi or Sembawa)—meaning there was no resting month when no tapping occurred. In tropical regions (latitude 8–20°), where there is a distinctly dry, wet, and cool season, tapping is stopped every year in February, March, and April (dry season), allowing nine months of tapping and three months of resting period [57,58]. For tropical regions (latitude > 20°) where there is a distinctly dry, wet, and cool season, and also experiencing hail events [54], rubber trees are usually tapped from May through November [38,48]. We combined the above information and set up the scheme for prescribing the tapping period at the site as follows:

$$\text{tapping}_{\text{period}} = \begin{cases} \text{all months for } |\text{latitude}| \leq 7^\circ \\ \text{months} \geq 5 \text{ or months} < 2 \text{ for } 7^\circ < \text{latitude} \leq 20^\circ \\ 5 \leq \text{months} \leq 11 \text{ for latitude} > 20^\circ \end{cases} \quad (10)$$

The implication of Equation (10) is that it facilitates changes in carbon allocation patterns of rubber plantations spatially.

2.8. Model Calibration

We did not use a formal optimization method to obtain the parameter values because we lacked data from which we could ascertain ranges for all parameters. Instead, we calibrated the model by looking at different processes one at a time (mostly), which means that for every process, we made some assumptions or had some logic. First, we tried to obtain reasonable phenology (leaf area index dynamics) based on four distinct ranges of latitudes. Second, to avoid more extended periods of leaf offset at latitudes away from the equator, we reduced the default value of critical soil water potential (from −0.8 to −2 MPa). Third, the default leaf longevity was about 0.48 years, which seemed low, so we increased it to 1 year. Fourth, the allocation ratio of stem to leaf from 2.3 is reduced to 1, where we assumed rubber trees allocate carbon similarly in leaves and stems. The second, third, and fourth changes were made simultaneously, and the model was run. Model outputs were compared with measurements.

We increased the multiplier factor (from 1 to 1.5) to increase litterfall rates in the dry season. We ran the model several times here because we changed the value in increments of 0.1 and compared the model values of litterfall against measurements. Ultimately we were able to arrive at the critical value, i.e., 1.5. The other calibrated parameters, ftap, dsladlai, and medlynslope, were jointly calibrated—meaning that we manually adjusted these three parameters together. The direction of change of these parameters was determined by comparing the model and measured values of latex yield and transpiration. The model

was then run, and model outputs were compared with measurements. We repeated this process several times until we arrived at their optimum values.

2.9. Rubber PFT Simulations and Evaluations

Using a clear-cut site disturbance implementation for Jambi (see above), a rubber PFT simulation in Jambi was performed for the period 2001 to 2014, where the parameters of the model (optimized parameter values; Table 1) were obtained either through field measurements or using model calibration methods [44,59]. See the rubber PFT development section for specific details about how the "optimized parameter values" of rubber were obtained. To evaluate rubber PFT simulations at other sites (SRC, CRRI, and Som Sanuk) that use the optimum parameter set values (Table 1), a rubber plantation simulation was performed for each site from their clear-cut year through the year 2014.

In this study, two different metrics were used to quantify model performance against the observed datasets. One is a model bias (MB) and the other is based on goodness-of-fit value (the R^2 value) [60,61]. MB was calculated as the mean of the model observation residuals [62]:

$$\mathrm{MB} = \overline{(\hat{y}_i - y_i)} \tag{11}$$

where y_i and $\hat{y}_i$ are the observed and model-simulated values, respectively.

A positive bias indicates that the model overestimated the observation data. The determination of coefficient of the ideal model is close to 1 (R^2 = 1 and MB = 0). If the modeled values yield an R^2 value close to 1, but a large bias, we can conclude that the model captured the dynamics of the processes, but relevant parameter values still need further refinement [27]. For instances where modeled values yield a bias close to 0 with a low R^2 value, we can conclude that the model does not adequately capture the dynamics of the processes [27], and in this case, a more realistic mechanism needs to be developed to improve the simulation. We present model evaluation for specific variables at individual sites when observation data are available because not every variable is measured at all the sites.

2.10. Comparing CLM-Rubber Model with Other Models

It is important to compare CLM-rubber model results with the existing model simulations from the literature. To this end, we collected data from the literature that performed modeling simulations. We found modeled data on net ecosystem exchange and latent heat flux from CRRI, Cambodia (11.6° N, 103.3° E; 57 m elevation) (SVAT-rubber model; [15]) and modeled latex harvest yield data from Neban Reserve (NR), China (22° N, 100° E; 680 m elevation) (LUCIA-rubber model; [16]). We performed CLM-rubber simulations at these two sites by essentially following a similar scheme as mentioned above and compared our results with the SVAT-rubber and LUCIA-rubber models.

3. Results

3.1. Rubber Modeled Using Alternate Tropical Forest Assumptions

At Jambi, Indonesia, when rubber was modeled as either AS_EVG or AS_DEC, both models predicted no change in seasonal leaf litterfall rates—this is contrary to the measurements (Figure 1a). AS_EVG or AS_DEC models predicted similar transpiration rates for June and August, respectively (~0.1 mm h^{-1}; Figure 1b). Compared to the measurements, the predicted transpiration rates using either AS_EVG or AS_DEC in June and August were more than 2-fold and 3-fold, respectively (see Figure 1b). In the case of the LAI, both the AS_EVG and the AS_DEC largely overestimated the measured LAI (see Figure 1c).

When rubber was modeled using either AS_EVG or AS_DEC at the SRC site in Indonesia, both models predicted no change in seasonal LAI values or no change in seasonal leaf carbon values—these contrast the measurements (Figure 2a,b). As in the case of Jambi, the LAI predicted by either AS_EVG or AS_DEC models largely overestimated the measured LAI and could not predict declines in either LAI values or leaf carbon values as measured (Figure 2a,b).

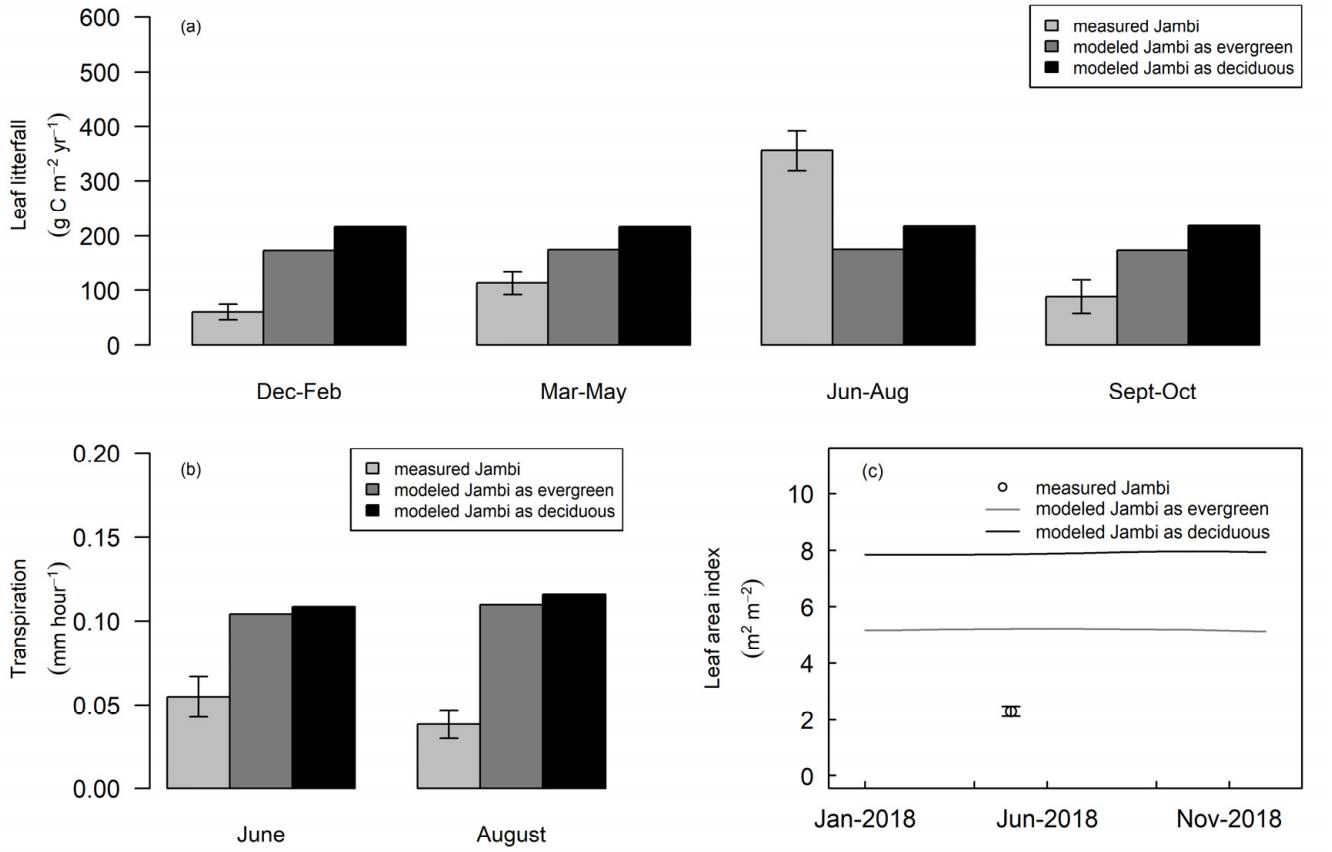

Figure 1. Seasonal trends of leaf litterfall (**a**) of rubber plants simulated by CLM (modeled using standard tropical evergreen parameters or standard tropical deciduous parameters) and measured values (bars are standard errors (n = 4 plots) during the mature phase of growth of smallholder rubber plantations in Jambi, Indonesia. Measured (bars indicate the standard errors) and CLM simulated monthly transpiration rates of June and August (**b**), and monthly values of leaf area index (**c**) (simulated by CLM (black line), measured values (open circles)) of rubber plantation in Jambi, Indonesia, are also shown. The measured data are taken from published studies [34,63,64].

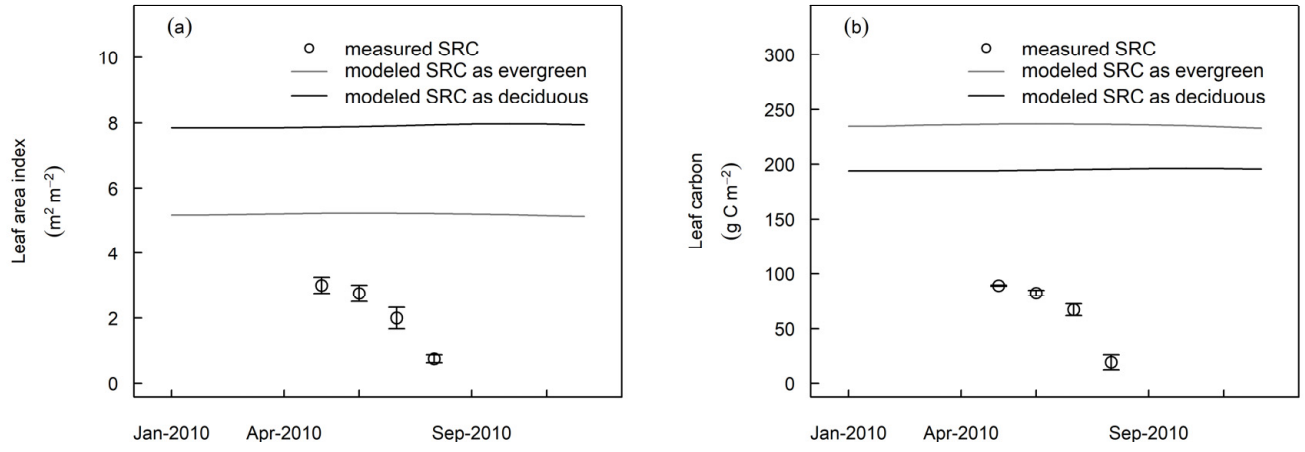

Figure 2. Measured (open circles, bars are standard errors) and CLM simulated (gray line, modeled using standard tropical evergreen parameters; black line, modeled using standard tropical deciduous parameters) leaf area index (**a**) and leaf carbon (**b**) of smallholder rubber plantations in 2013 in SRC, Indonesia. The measured data are taken from a published study [55].

At CRRI, Cambodia, both the AS_EVG or AS_DEC models could not predict seasonal changes in LAI (Figure 3a). In particular, both of these models could not predict the correct timing of the leaf offset (Figure 3a). Thus there was a considerable delay in the timing of defoliation and refoliation (Figure 3a). As for evapotranspiration, AS_EVG and AS_DEC models could not capture the measurements during the refoliation period (Figure 3b). Both AS_EVG and AS_DEC models predicted a similar value of CO_2 uptake from the atmosphere and also predicted lower CO_2 uptake compared to the field measurements (Figure 3c).

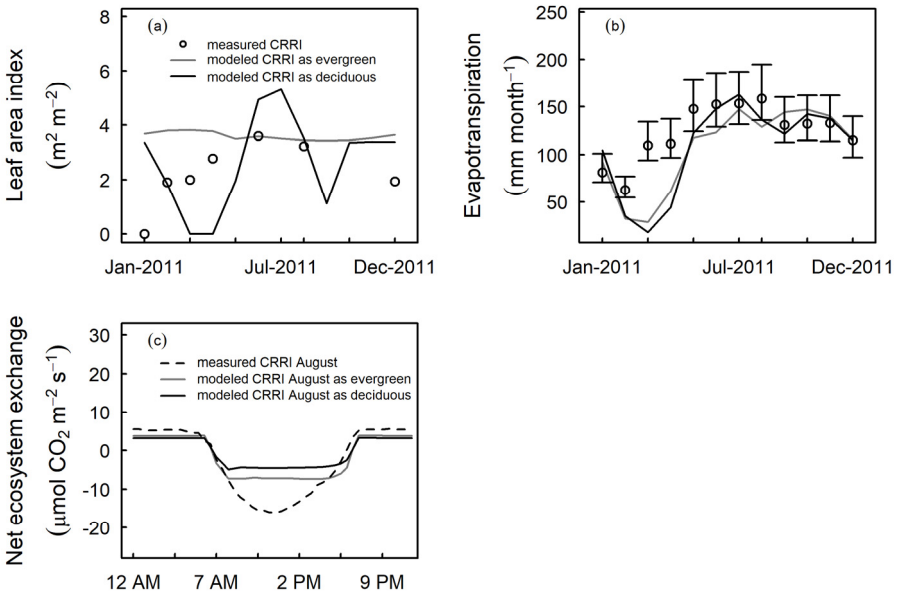

Figure 3. Monthly values of leaf area index (**a**) and evapotranspiration (**b**) of rubber plantations simulated by CLM (gray line, modeled using standard tropical evergreen parameters; black line, modeled using standard tropical deciduous parameters) and measured values (open circles; bars indicate the standard errors) during the mature phase of growth of rubber. Diel variations of net ecosystem exchange (**c**) of rubber plantations simulated by CLM (gray line, modeled using standard tropical evergreen parameters; black line, modeled using standard tropical deciduous parameters) and measured values (dashed lines) in CRRI, Cambodia in 2011 are also shown. All of the measured data are taken from published studies [10,15].

At the Som Sanuk site in Thailand, both the AS_EVG or AS_DEC models overestimated LAI and could not predict seasonal changes in LAI (Figure 4a). AS_EVG and AS_DEC models could not capture evapotranspiration measurements, especially during the refoliation period (Figure 4b). AS_EVG and AS_DEC models predicted lower CO_2 uptake than the measurements (Figure 4c).

3.2. Phenology of Rubber in Jambi

Our newly developed and parameterized CLM-rubber PFT can simulate the seasonal patterns of leaf litterfall comparable to measurements in Jambi (Figure 5a), including the increase and decline of leaf litterfall during a year (Figure 5a). The magnitude of the observed transpiration values was better captured by the model in August than June (Figure 5b). For June, the model overestimated the observed transpiration mean value by 0.025 mm h^{-1}. The value of LAI predicted by the model was slightly higher than the one-time observed value in Jambi (Figure 5c). The model predicted considerable changes in monthly LAI values (Figure 5c) in Jambi. On the annual time scale, the model slightly overestimated net primary productivity by about 8% (Figure 6a) and underestimated fine root biomass by about 10% (Figure 6c). In comparison, the model matched well with the measurements of latex yield (Figure 6b) and soil moisture (Figure 6d).

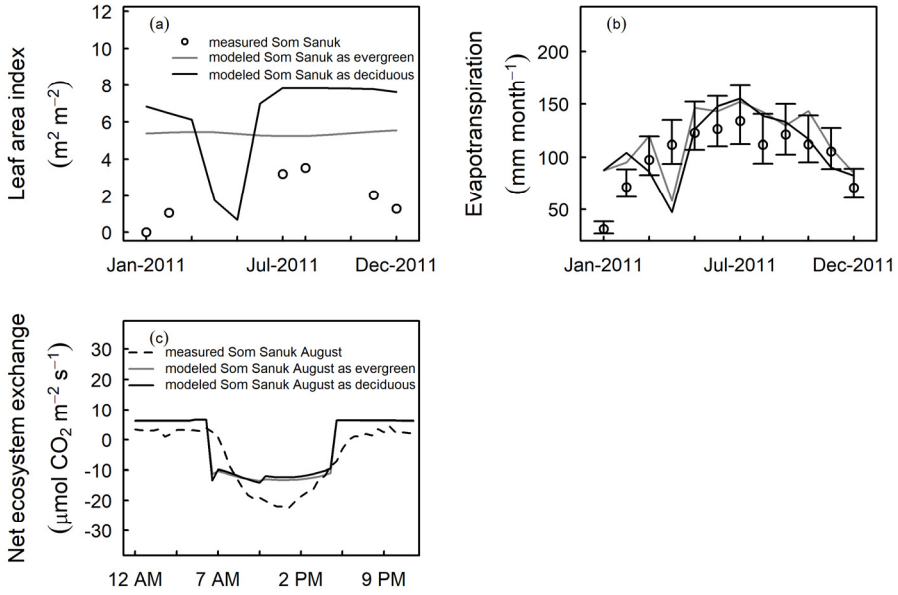

Figure 4. Monthly values of leaf area index (**a**) and evapotranspiration (**b**) of rubber plantations simulated by CLM (gray line; modeled using standard tropical evergreen parameters; black line, modeled using standard tropical deciduous parameters) and measured values (open circles; bars indicate the standard errors) during the mature phase of growth of rubber. Diel variations of net ecosystem exchange (**c**) of rubber plantations simulated by CLM (gray line, modeled using standard tropical evergreen parameters; black line, modeled using standard tropical deciduous parameters) and measured values (dashed lines) in Som Sanuk, Thailand, in 2009 are also shown. All of the measured data are taken from published studies [10] except for net ecosystem exchange, which is digitized from a leaflet (https://lcluc.umd.edu/sites/default/files/lcluc_documents/Fox_1.pdf, accessed on 12 December 2021).

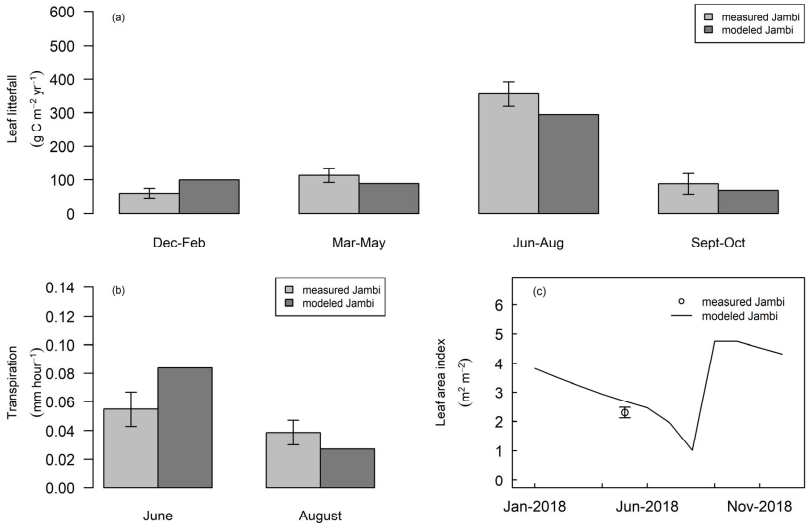

Figure 5. Seasonal trends of leaf litterfall (**a**) of rubber plants simulated by CLM-rubber (modeled using rubber parameters) and measured values (bars are standard errors (n = 4 plots)) during the mature phase of growth of smallholder rubber plantations in Jambi, Indonesia. Measured (bars indicate the standard errors) and CLM-rubber simulated monthly transpiration rates of June and August (**b**), and monthly values of leaf area index (**c**) (simulated by CLM-rubber (black line), measured values (open circles)) of rubber plantation in Jambi, Indonesia, are also shown. Values of model bias and goodness-of-fit are specified as MB and R^2, respectively. The measured data are taken from published studies [34,63,64].

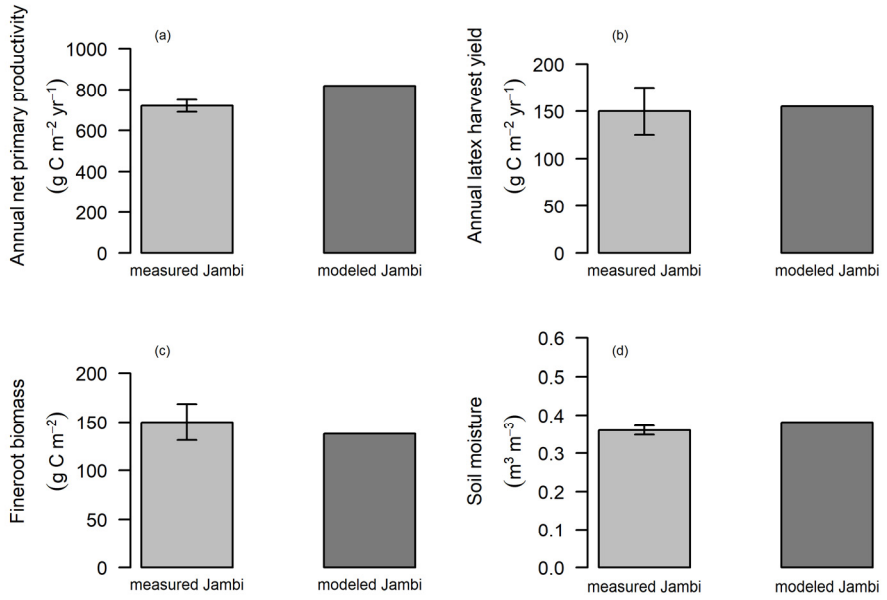

Figure 6. Measured (bars are standard error, n = 4 plots) and CLM-rubber (modeled using rubber parameters) net primary productivity (**a**), latex yield (**b**), fine root biomass (**c**), and soil moisture in the top 5 cm soil depth (**d**) of smallholder rubber plantations in 2013 in Jambi, Indonesia. The measured data are taken from published studies [42,65].

3.3. Model Evaluation at Independent Sites

In agreement with empirical observation, the model predicted the seasonal trends in LAI, leaf carbon, and latex yield in SRC, Indonesia, reasonably well (Figure 7a–c). The model had a negative bias for LAI and leaf carbon (Figure 7a,b), but these biases were relatively low. At the same site, the model explained 43% of the variability in the measured latex yield (Figure 7c), and it predicted an overestimate of latex yield of 5.12 g C m^{-2} yr^{-1} (Figure 7c).

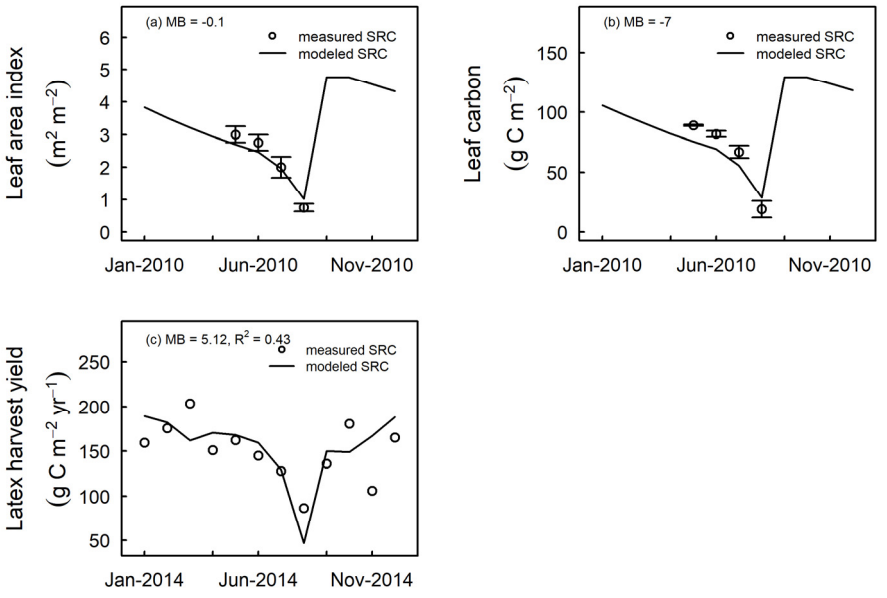

Figure 7. Monthly values of leaf area index (**a**), leaf carbon (**b**), and latex yield (**c**) of rubber plantations simulated by CLM-rubber (black line) and measured values (open circles) during the mature phase of growth of rubber plantation in SRC, Indonesia. Values of model bias and goodness-of-fit are specified as MB and R^2, respectively. The measured data are taken from published studies [14,55].

When evaluated at the site with eddy covariance measurements in rubber plantations (CRRI, Cambodia), the model generally captured the seasonal variations and magnitude of LAI (Figure 8a; R^2 = 0.53, *p*-value < 0.05), evapotranspiration (Figure 8b; R^2 = 0.58, *p*-value < 0.05) and net ecosystem exchange of CO_2 (Figure 8c; R^2 = 0.96, *p*-value < 0.05). Relative to measurements, the magnitude of the LAI was overestimated more at the Som Sanuk site (Figure 9a; model bias = 0.43) than at the CRRI site (Figure 8a; model bias = −0.02). However, by looking closely at the figure plots for LAI between the sites (Figure 8a vs. Figure 9a), it may seem the opposite. That is, the modeled LAI appears to be better fitted to measurements at the Som Sanuk site than CRRI site (Figure 8a vs. Figure 9a). The reason is at the CRRI site, the modeled LAI both over predicts as well as under predicts monthly LAI values (Figure 8a) so the overall model bias is much reduced at this site. Between 10 am and 3 pm, there were larger differences between the modeled and measured net ecosystem exchange at Som Sanuk (Figure 9c) than at CRRI (Figure 8c), but the overall explanatory power of the model for the measured net ecosystem exchange at Som Sanuk and CRRI was relatively high; R^2 = 0.8 at Som Sanuk (Figure 9c) and R^2 = 0.96 at CRRI (Figure 8c).

3.4. Comparing CLM-Rubber Model with Other Models

At CRRI, Cambodia, CLM-rubber and SVAT-rubber models explained a similar amount of variation in measured diel net ecosystem exchange (Figure 10a) and measured diel latent heat fluxes (Figure 10b). Still, the explanatory power of the CLM-rubber was slightly better than the SVAT-rubber. SVAT-rubber predicted a considerable amount of temporal variability—both for net ecosystem exchange and latent heat flux (Figure 10a,b). At Neban reserve, China, CLM-rubber performed similar to the LUCIA-rubber by capturing the seasonality and magnitudes of the latex harvest yield values (Figure 10c).

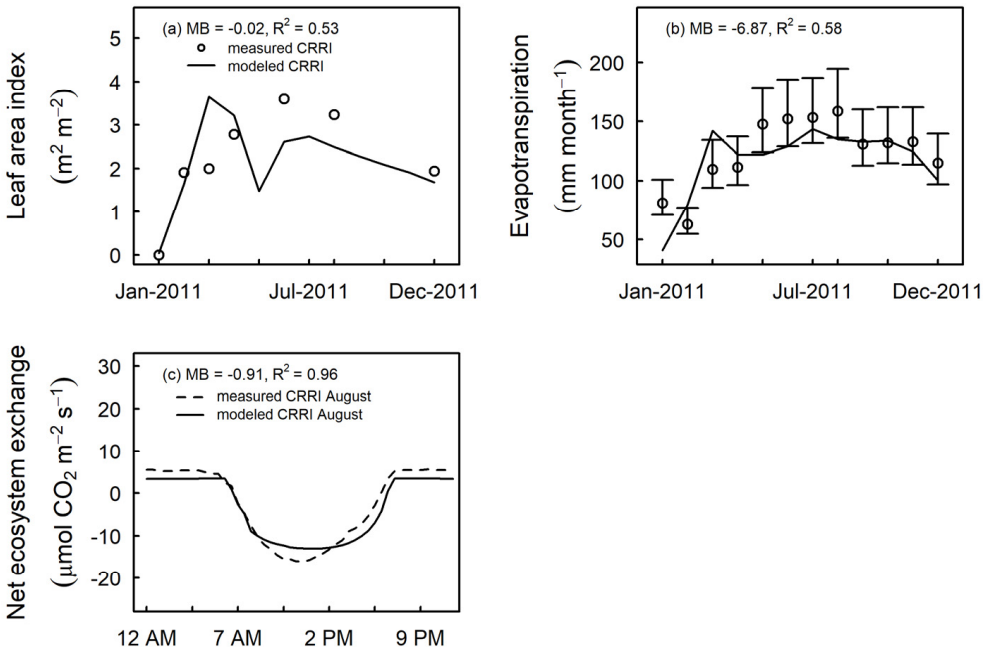

Figure 8. Monthly values of leaf area index (**a**) and evapotranspiration (**b**) of rubber plantations simulated by CLM-rubber (solid lines) and measured values (open circles; bars indicate the standard errors) during the mature phase of growth of rubber. Diel variations of net ecosystem exchange (**c**) of rubber plantations simulated by CLM-rubber (solid lines) and measured values (dashed lines) in CRRI, Cambodia, in 2011 are also shown. Values of model bias and goodness-of-fit are specified as MB and R^2, respectively. All of the measured data are taken from published studies [10,15].

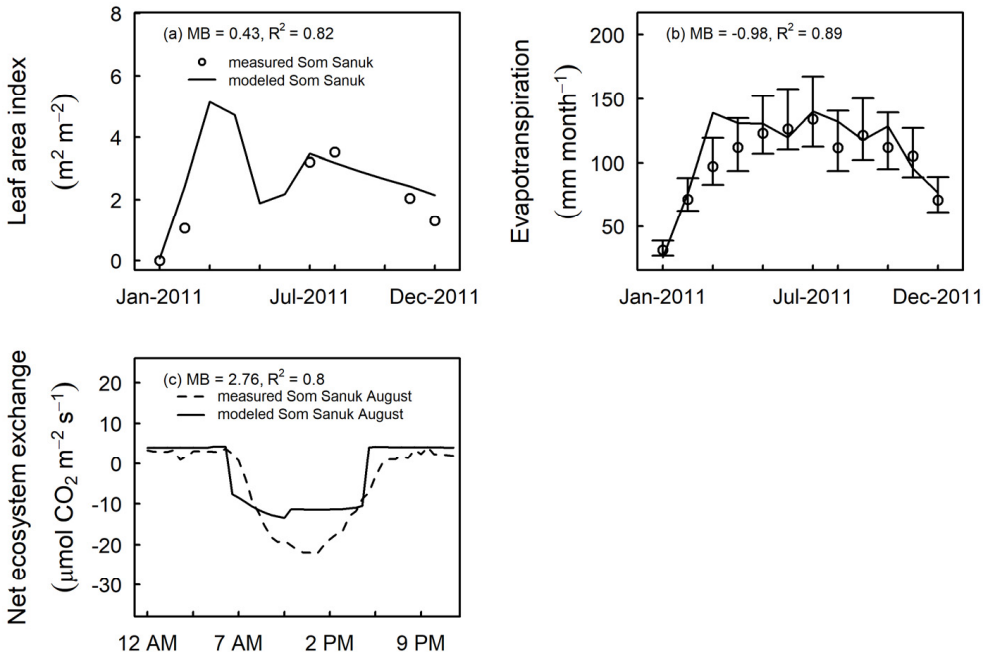

Figure 9. Monthly values of leaf area index (**a**) and evapotranspiration (**b**) of rubber plantations simulated by CLM-rubber (solid lines) and measured values (open circles; bars indicate the standard errors) during the mature phase of growth of rubber. Diel variations of net ecosystem exchange (**c**) of rubber plantations simulated by CLM-rubber (solid lines) and measured values (dashed lines) in Som Sanuk, Thailand, in 2009 are also shown. Values of model bias and goodness-of-fit are specified as MB and R^2, respectively. All of the measured data are taken from published studies [10] except for NEE, which is digitized from a leaflet (https://lcluc.umd.edu/sites/default/files/lcluc_documents/Fox_1.pdf, accessed on 5 March 2019).

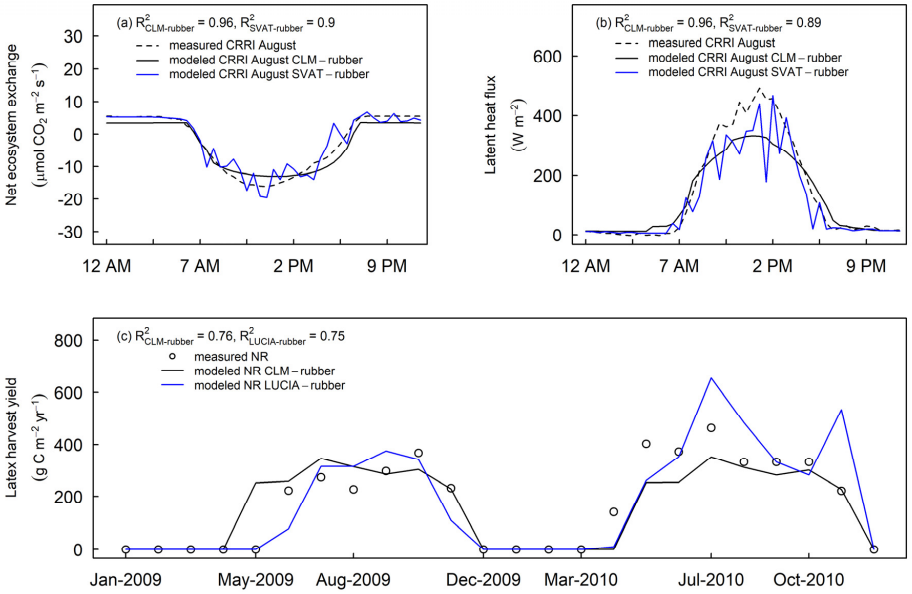

Figure 10. Diel variations of net ecosystem exchange (**a**) and latent heat flux (**b**) of rubber plantations simulated by CLM-rubber (solid black line) and SVAT-rubber (solid blue line), and measured values (dashed line) in CRRI, Cambodia, in 2011. Values of goodness-of-fit for CLM-rubber, SVAT-rubber, and LUCIA-rubber are specified as $R^2_{\text{CLM-rubber}}$, $R^2_{\text{SVAT-rubber}}$, and $R^2_{\text{LUCIA-rubber}}$, respectively. Monthly values of latex harvest yield (**c**) of rubber plantations simulated by CLM-rubber (solid black line) and LUCIA-rubber (solid blue line), and measured values (open circles) in NR, China, between 2009 and 2010. All of the measured data are taken from published studies [10,15,16].

4. Discussion

Our modeling efforts aimed to simulate the phenology, allocation, and latex yield of rubber plantations from Southeast Asia using CLM5. We show that the newly developed rubber PFT and related parametrization outperforms the baseline parametrization of tropical evergreen or the baseline tropical deciduous PFTs in CLM5 for simulating the leaf area index, carbon, and water fluxes of rubber plantations. Our modeling work shows that daylength can be used as a universal trigger for defoliation and refoliation of rubber plantations. Our model can predict reasonable seasonal patterns of latex yield despite highly variable tapping periods across Southeast Asia. Finally, we show that CLM-rubber performs similar in simulating carbon and energy fluxes to the existing rubber model simulations available in the literature.

4.1. Tropical Evergreen and Deciduous Simulations

For rubber plantations growing at latitudes lower than 8°, the model that used baseline tropical evergreen or the baseline tropical deciduous functions and parameterization could not predict the seasonality of litterfall because the rate coefficient for background litterfall was invariant over the seasons. The seasonality of LAI and leaf carbon by both forest types models were also not properly simulated at these sites because the modeled soil water was not low enough to trigger the leaf offset. The magnitudes of LAI and leaf carbon were also primarily overestimated. The likely reasons include parameters related to photosynthesis, e.g., stomatal conductance and parameters related to plant growth, such as specific leaf area [28]. Additionally, how fast specific leaf area changes relative to the change in leaf area index and how much carbon is allocated to different tissues, such as the ratio of stem: leaf [31], can attribute to overestimation of LAI and leaf carbon.

For rubber plantations growing at latitudes greater than 8°, the model that used baseline tropical evergreen or the baseline tropical deciduous functions and parameterization could not predict the proper seasonality of LAI. However, the model that used baseline tropical deciduous functions and parameterizations was better in predicting the seasonal patterns of LAI than the model that used baseline tropical evergreen functions and parameterization. The reason for this discrepancy is that former model was able to trigger leaf offset as the modeled soil water reached low values; however, the timing and the duration of the leaf offset were not accurate. In the growing season, sometimes both models predicted reduced LAI, and this result was due to low irradiance, as rainfall was high during this period in both model simulations.

4.2. Daylength, Carbon, and Water Fluxes

We demonstrated in this study that increasing the background litterfall rate enables modeling of the seasonal cycle of leaf litterfall rates in Jambi, Indonesia. The observed seasonality of leaf litterfall could be controlled by a combination of climatic factors or soil conditions. Our model predicted the peak of the monthly leaf litterfall rate at Neban reserve, China, as February, and this modeled result is in agreement with a rubber plantation in China [38], where January is typically the coldest month, and leaf shedding occurs after the coldest month [38]. These results indicate that CLM-rubber will predict reasonably well the seasonality of leaf litterfall of rubber plantations across Southeast Asia.

Our modeling work shows that daylength can be sufficient to represent regional heterogeneity for both the leaf offset and leaf onset of rubber plantations. Daylength works not only for sites with a pronounced dry season [10], but also for sites in Indonesia where soil moisture may never drop to a critical level. Since rubber plantations are facultative deciduous or semideciduous, we are confident that daylength, as implemented in our study, can be directly used for simulating phenological cycles for other facultative deciduous ecosystems (semideciduous) from Southeast Asia that are managed, such as teak plantations [66] and cocoa plantations [67]. Additionally, daylength can also be implemented in CLM5 to potentially improve simulations of unmanaged ecosystems such as semievergreen natural forests in Thailand [68].

The magnitude of the monthly latex yield simulated by CLM-rubber matched quite well with the observations at the independent sites: the SRC site (Indonesia) and at the Neban reserve site (China). This was an unexpected result because we did not consider tapping frequency in the model. We are aware that tapping frequency generally varies among plantations—two tapping days and one resting day or one tapping day and two resting days [10]; in the model, we assumed that the proportion of tapping assimilate allocation is constant.

The relatively high R^2 values of modeled evapotranspiration rates at the evaluation sites suggest that the model captured the dynamics of processes. Overall, CLM-rubber was able to capture the average trend of carbon and water fluxes of various rubber plantations (R^2~0.73, p-value < 0.05), which meets the general purpose for representing a PFT in a land surface scheme.

4.3. Intermodel Comparisons

We compared the simulations of CLM-rubber with simulations of SVAT-rubber and LUCIA-rubber. We also evaluated these models against field observations at the CRRI and Neban sites. CLM-rubber successfully captured the trend of net ecosystem exchange and latent heat flux at the CRRI site because it has the improved seasonal cycle of leaf onset/offset. SVAT-rubber better captured the magnitude of these fluxes (at times) compared to CLM-rubber because it was initialized by prescribing the initial value of LAI as 3.89 m^2 m^{-2} [15], which is almost the peak value of measured LAI for rubber plantations.

CLM-rubber captured the seasonality of latex yield at Neban reserve because CLM-rubber was able to allocate carbon to different tissues properly, and it also predicted the proper leaf shedding period. On the other hand, LUCIA-rubber predicted delayed leaf flushing (shown to be up to a 2 month delay) and subsequently underestimated latex yield [16]. Our model comparisons indicate that CLM-rubber generally performs similar to the other two models—this highlights that the modeling efforts for rubber in CLM are viable and valuable.

5. Conclusions

The overarching objective of this study was to simulate leaf area index and carbon and water fluxes of rubber plantations from Southeast Asia using CLM5. We found that the baseline tropical evergreen or the baseline tropical deciduous functions and parameterization that are commonly used for carbon and water flux parameterization in region models cannot be directly used to simulate the leaf area index and carbon and water fluxes of rubber plantations. By using daylength as a trigger for both defoliation and refoliation, prescribing tapping period, and using appropriate parameterization, the developed model (CLM-rubber) was capable of capturing the magnitude and seasonality of carbon and water fluxes at different sites in Southeast Asia. These findings suggest that CLM-rubber could be applied to the Southeast Asian region to examine the spatiotemporal variations in carbon and water fluxes for rubber plantations under climate change and estimate the impact of land-use change driven by rubber expansion on the regional carbon balance and water resources, and the impact of potential feedbacks to climate.

Author Contributions: Conceptualization, A.A.A., Y.F., E.V. and A.K.; methodology, A.A.A. and Y.F.; software, A.A.A. and Y.F.; validation, A.A.A.; formal analysis, A.A.A.; investigation, A.A.A. and Y.F.; data curation, M.D.C., M.M.K., E.P.-H., A.N.C., C.S., A.R. (Alexander Röll) and A.M.; writing—original draft preparation, A.A.A.; writing—review and editing, A.A.A., Y.F., M.D.C., M.M.K., E.P.-H., A.N.C., F.E.M., C.S., A.R. (Alexander Röll), A.M., A.O., A.R. (Andre Ringeler), C.L., R.A., T.J., S.T., H.K., D.H., C.X., C.D.K., K.D., R.A.F., E.V. and A.K.; visualization, A.A.A. and A.R. (Andre Ringeler); supervision, F.E.M., E.V. and A.K.; project administration, T.J.; funding acquisition, T.J., S.T., E.V. and A.K. All authors have read and agreed to the published version of the manuscript.

Funding: This research was funded by the Deutsche Forschungsgemeinschaft (DFG, German Research Foundation) grant number 192626868 and the APC was funded by the same grant number.

Institutional Review Board Statement: Not applicable.

Informed Consent Statement: Not applicable.

Data Availability Statement: The data for CLM-rubber used in this paper can be found on Zenodo at https://doi.org/10.5281/zenodo.4729044 accessed on 12 December 2021 (Ali et al., 2021a). Interested users can download the version of CLM5 used in this study from here https://github.com/ESCOMP/ctsm, accessed on 12 December 2021.

Acknowledgments: We gratefully acknowledge financial support from the Deutsche Forschungsgemeinschaft (DFG, German Research Foundation)—project number 192626868—CRC 990 and the Ministry of Research, Technology, and Higher Education (Ristekdikti) in the framework of the collaborative German–Indonesian research project CRC990, subproject A07. We thank the authors of Giambelluca et al. (2016) for providing the climate data. C.X. acknowledges support from DOE's Next Generation Ecosystem Experiment (NGEE)—Tropics project. Finally, we thank the village leaders and farmers for allowing us to conduct our research on their land.

Conflicts of Interest: The authors declare no conflict of interest.

Appendix A

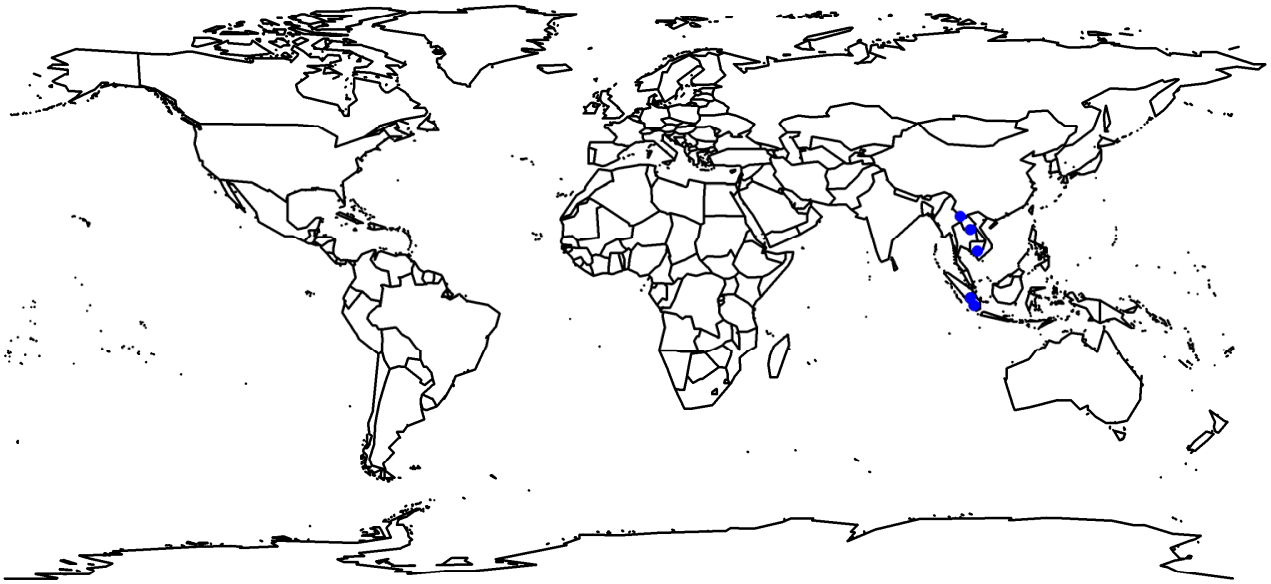

Figure A1. The spatial location of the five Southeast Asian sites indicated by blue points. The model was either developed or evaluated at these sites.

Appendix B. Leaf Onset/Offset Parameterization

For the standard stress deciduous phenology, leaf onset is determined by soil wetness. At the end of the previous offset period, an accumulated soil water index (SWI) is set to zero, and accumulation is calculated as

$$SWI^n = \begin{cases} SWI^{n-1} + f_{day} \text{ for } \varphi_{soil_3} \geq \varphi_{threshold} \\ SWI^{n-1} \text{ for } \varphi_{soil_3} < \varphi_{threshold} \end{cases} \quad \text{(A1)}$$

where n and $n-1$ refer to the values in the previous and current time steps, φ_{soil_3} is the soil water potential (MPa) in the third soil layer (6.23–9.06 cm), $\varphi_{threshold}$ is -0.8 MPa, and f_{day} is a time step (30 min in CLM5) as a fraction of a day. Onset is triggered when SWI exceeds 15 days [39]. Onset is also triggered when the daylength is greater than 6 h, or when the accumulated number of growing-degree-days (which is based on the soil temperature) exceeds a threshold value.

The offset soil wetness index (OSWI) begins accumulating time steps once the previous leaf onset phase is complete. The algorithm differs slightly from the onset trigger in that OSWI can increase or decrease, as described below:

$$OSWI^n = \begin{cases} OSWI^{n-1} + f_{day} \text{ for } \varphi_{soil_3} \leq \varphi_{threshold} \\ \max(OSWI^{n-1} - f_{day}\ ,\ 0) \text{ for } \varphi_{soil_3} > \varphi_{threshold} \end{cases}, \quad (A2)$$

where $\varphi_{threshold}$ is -0.8 MPa, and leaf offset is triggered when OSWI equals 15 days. Offset is also triggered when the daylength is shorter than 6 hours, or when there is a sustained period of cold temperatures.

Appendix C. Background Leaf Litterfall

The background leaf litterfall rate occurs at a slow rate over an extended period of time. The offset period litterfall or the background litterfall mechanism may be active, but not both at once. When plant stresses occur less frequently than once per year, leaf offsets are not met for one year or longer. This condition is evaluated by tracking the number of days since the beginning of the most recent onset period (n_{days_active}, d). At the end of an offset period, n_{days_active} is reset to 0. A long growing season control variable (LGS, range 0 to 1) is calculated as:

$$LGS = \begin{cases} 0 & \text{for } n_{days\_active} < 365 \\ \left(n_{days\_active}/365\right) - 1 & \text{for } 365 \leq n_{days\_active} < 730 \\ 1 & \text{for } n_{days\_active} \geq 730 \end{cases}. \quad (A3)$$

The rate coefficient for background litterfall (r_{bglf}, s^{-1}) is calculated as a function of LGS:

$$r_{bglf} = \frac{LGS}{\gamma_{leaf \cdot 365 \cdot 86{,}400}} \quad (A4)$$

where γ_{leaf} is the leaf longevity. The result is a shift to continuous litterfall as n_{days_active} increases from 365 to 730. When a new offset period is triggered r_{bglf} is set to 0. The offset period (complete defoliation) litterfall carbon fluxes of the leaf ($CF_{leaf,litter}$, gC $m^{-2}s^{-1}$) is calculated as follows:

$$CF_{leaf,litter} = (CS_{leaf}/\Delta t) + CF_{alloc,leaf\_tot} \quad (A5)$$

where CS_{leaf} (gC m^{-2}) is the leaf carbon from the storage pool, Δt is the time step (s), and $CF_{alloc,leaf\_tot}$ ($gCm^{-2}s^{-1}$) is the total allocation to a new leaf. When there is only background litterfall, given a specification of the background litterfall rate (r_{bglf}, s^{-1}), then litterfall carbon fluxes of the leaf are calculated as

$$CF_{leaf,litter} = r_{bglf} CS_{leaf} \quad (A6)$$

Appendix D. Allocation

Latex harvest yield for rubber is based on modifying the carbon allocation scheme in CLM5 (Lawrence et al., 2019). As is the case of the phenology scheme, we first describe the standard carbon allocation scheme and then describe the changes we made in this scheme for rubber. CLM5 calculates carbon allocated to new growth, based on five allometric parameters that relate allocation between tissue types [69]: (1) ratio of new fine roots to new leaf carbon allocation (a_1); (2) ratio of new coarse roots to new stem carbon allocation (a_2); (3) wood allocation, the ratio of new stems to new leaf carbon allocation (a_3); (4) ratio of new live wood to new total wood allocation (a_4); and (5) ratio of growth respiration carbon to new growth carbon (g_1). Most of these allometric parameters are constants for natural PFTs in CLM5 (e.g., $a_1 = 1$, $a_2 = 0.3$, $a_3 = 2.3$, $a_4 = 0.1$, and $g_1 = 0.3$ for the broadleaf

deciduous tropical PFT). For natural woody PFTs, the parameter a_4 is used to partition total stem allocation to livewood and deadwood pools.

Given the above allocation parameters (a_1, a_2, a_3, a_4, and g_1), the total carbon allocation to new growth $\left(CF_{alloc},\ gC\ m^{-2}s^{-1}\right)$ can be expressed as a function of new leaf carbon allocation $\left(CF_{GPP,leaf},\ gC\ m^{-2}s^{-1}\right)$:

$$CF_{alloc} = CF_{GPP,leaf}C_{allom}, \tag{A7}$$

where C_{allom} is the carbon allocation allometry [70], which is defined as follows:

$$C_{allom} = (1 + g_1)(1 + a_1 + a_3(1 + a_2)) \tag{A8}$$

Total allocation to new leaf carbon $\left(CF_{alloc,leaf\_tot}, gC\ m^{-2}s^{-1}\right)$ is calculated as:

$$CF_{alloc,leaf\_tot} = \frac{CF_{alloc}}{C_{allom}} \tag{A9}$$

In CLM5, we note that for all deciduous PFTs, there is a fraction of allocation that goes into the growth pool (fcur), which is currently set to 0 (unitless) and the remainder (1- fcur) goes to the storage pool. Subsequently, the deciduous phenology module either uses the onset growth function or a background growth transfer rate (bgtr; outside of onset period) to move storage carbon to displayed growth pools. There are two carbon pools associated with each plant tissue in CLM5: (1) growth and (2) storage. The carbon pools that represent growth include carbon in leaf (leafc), carbon in fine roots (frootc), carbon in live stem (livestemc), carbon in dead stem (deadstemc), carbon in live coarse roots (livecrootc), and carbon in dead coarse roots (deadcrootc). The carbon pools that represent storage have a suffix "_storage" and include leafc_storage, frootc_storage, livestemc_storage, deadstemc_storage, livecrootc_storage, and deadcrootc_storage terms. In CLM5, the carbon allocation fluxes have a prefix "cpool_to_".

For CLM5, we show below some key carbon allocation fluxes for the livestem and deadstem pools. Given $CF_{alloc,leaf\_tot}$, and fcur, the allocation fluxes of carbon to growth and storage pools for the various tissue types can be calculated as follows:

$$\text{cpool\_to\_livestemc} = CF_{alloc,leaf\_tot} \cdot a_3 \cdot a_4 \cdot \text{fcur}, \tag{A10}$$

$$\text{cpool\_to\_livestemc\_storage} = CF_{alloc,leaf\_tot} \cdot a_3 \cdot a_4 \cdot (1 - \text{fcur}) \tag{A11}$$

$$\text{cpool}_{to_{deadstemc}} = CF_{alloc,leaf_{tot}} \cdot a_3 \cdot (1 - a_4) \cdot \text{fcur}, \tag{A12}$$

$$\text{cpool\_to\_deadstemc\_storage} = CF_{alloc,leaf\_tot} \cdot a_3 \cdot (1 - a_4) \cdot (1 - \text{fcur}) \tag{A13}$$

The nitrogen pools follow the stoichiometric relationship with carbon pools. More details can be found in Lawrence et al. [31].

References

1. De Blécourt, M.; Brumme, R.; Xu, J.; Corre, M.D.; Veldkamp, E. Soil Carbon Stocks Decrease following Conversion of Secondary Forests to Rubber (*Hevea brasiliensis*) Plantations. *PLoS ONE* **2013**, *8*, e69357. [CrossRef] [PubMed]
2. Röll, A.; Niu, F.; Meijide, A.; Ahongshangbam, J.; Ehbrecht, M.; Guillaume, T.; Gunawan, D.; Hardanto, A.; Hendrayanto; Hertel, D.; et al. Transpiration on the rebound in lowland Sumatra. *Agric. For. Meteorol.* **2019**, *274*, 160–171. [CrossRef]
3. Ziegler, A.D.; Fox, J.M.; Xu, J. The Rubber Juggernaut. *Science* **2009**, *324*, 1024–1025. [CrossRef] [PubMed]
4. Hurni, K.; Schneider, A.; Heinimann, A.; Nong, D.H.; Fox, J. Mapping the Expansion of Boom Crops in Mainland Southeast Asia Using Dense Time Stacks of Landsat Data. *Remote Sens.* **2017**, *9*, 320. [CrossRef]
5. Senf, C.; Pflugmacher, D.; Van Der Linden, S.; Hostert, P. Mapping Rubber Plantations and Natural Forests in Xishuangbanna (Southwest China) Using Multi-Spectral Phenological Metrics from MODIS Time Series. *Remote Sens.* **2013**, *5*, 2795–2812. [CrossRef]

6. Drescher, J.; Rembold, K.; Allen, K.; Beckschäfer, P.; Buchori, D.; Clough, Y.; Faust, H.; Fauzi, A.M.; Gunawan, D.; Hertel, D.; et al. Ecological and socio-economic functions across tropical land use systems after rainforest conversion. *Philos. Trans. R. Soc. B Biol. Sci.* **2016**, *371*, 20150275. [CrossRef]
7. Lin, Y.; Zhang, Y.; Zhao, W.; Dong, Y.; Fei, X.; Song, Q.; Sha, L.; Wang, S.; Grace, J. Pattern and driving factor of intense defoliation of rubber plantations in SW China. *Ecol. Indic.* **2018**, *94*, 104–116. [CrossRef]
8. Kositsup, B.; Kasemsap, P.; Thanisawanyangkura, S.; Chairungsee, N.; Satakhun, D.; Teerawatanasuk, K.; Ameglio, T.; Thaler, P. Effect of leaf age and position on light-saturated CO_2 assimilation rate, photosynthetic capacity, and stomatal conductance in rubber trees. *Photosynthetica* **2010**, *48*, 67–78. [CrossRef]
9. Kositsup, B.; Montpied, P.; Kasemsap, P.; Thaler, P.; Améglio, T.; Dreyer, E. Photosynthetic capacity and temperature responses of photosynthesis of rubber trees (*Hevea brasiliensis* Müll. Arg.) acclimate to changes in ambient temperatures. *Trees* **2008**, *23*, 357–365. [CrossRef]
10. Giambelluca, T.W.; Mudd, R.G.; Liu, W.; Ziegler, A.D.; Kobayashi, N.; Kumagai, T.; Miyazawa, Y.; Lim, T.K.; Huang, M.; Fox, J.; et al. Evapotranspiration of rubber (*Hevea brasiliensis*) cultivated at two plantation sites in Southeast Asia. *Water Resour. Res.* **2016**, *52*, 660–679. [CrossRef]
11. Kumagai, T.; Mudd, R.G.; Giambelluca, T.; Kobayashi, N.; Miyazawa, Y.; Lim, T.K.; Liu, W.; Huang, M.; Fox, J.; Ziegler, A.D.; et al. How do rubber (*Hevea brasiliensis*) plantations behave under seasonal water stress in northeastern Thailand and central Cambodia? *Agric. For. Meteorol.* **2015**, *213*, 10–22. [CrossRef]
12. Allen, K.; Corre, M.D.; Tjoa, A.; Veldkamp, E. Soil Nitrogen-Cycling Responses to Conversion of Lowland Forests to Oil Palm and Rubber Plantations in Sumatra, Indonesia. *PLoS ONE* **2015**, *10*, e0133325. [CrossRef] [PubMed]
13. van Straaten, O.; Corre, M.D.; Wolf, K.; Tchienkoua, M.; Cuellar, E.; Matthews, R.B.; Veldkamp, E. Conversion of lowland tropical forests to tree cash crop plantations loses up to one-half of stored soil organic carbon. *Proc. Natl. Acad. Sci. USA* **2015**, *112*, 9956–9960. [CrossRef] [PubMed]
14. Cahyo, A.N.; Babel, M.S.; Datta, A.; Prasad, K.C.; Clemente, R. Evaluation of Land and Water Management Options to Enhance Productivity of Rubber Plantation Using Wanulcas Model. *AGRIVITA J. Agric. Sci.* **2016**, *38*, 93–102. [CrossRef]
15. Kumagai, T.; Mudd, R.G.; Miyazawa, Y.; Liu, W.; Giambelluca, T.W.; Kobayashi, N.; Lim, T.K.; Jomura, M.; Matsumoto, K.; Huang, M.; et al. Simulation of canopy CO_2/H_2O fluxes for a rubber (*Hevea brasiliensis*) plantation in central Cambodia: The effect of the regular spacing of planted trees. *Ecol. Model.* **2013**, *265*, 124–135. [CrossRef]
16. Yang, X.; Blagodatsky, S.; Marohn, C.; Liu, H.; Golbon, R.; Xu, J.; Cadisch, G. Climbing the mountain fast but smart: Modelling rubber tree growth and latex yield under climate change. *For. Ecol. Manag.* **2019**, *439*, 55–69. [CrossRef]
17. Liu, S.-J.; Zhou, G.-S.; Fang, S.-B.; Zhang, J.-H. Effects of future climate change on climatic suitability of rubber plantation in China. *Ying Yong Sheng Tai Xue Bao* **2015**, *26*, 2083–2090.
18. Hazir, M.H.M.; Kadir, R.A.; Karim, Y.A. Projections on future impact and vulnerability of climate change towards rubber areas in Peninsular Malaysia. *IOP Conf. Ser. Earth Environ. Sci.* **2018**, *169*, 012053. [CrossRef]
19. Ray, D.; Behera, M.; Jacob, J. Predicting the distribution of rubber trees (*Hevea brasiliensis*) through ecological niche modelling with climate, soil, topography and socioeconomic factors. *Ecol. Res.* **2016**, *31*, 75–91. [CrossRef]
20. Lang, R.; Goldberg, S.; Blagodatsky, S.; Piepho, H.; Harrison, R.D.; Xu, J.; Cadisch, G. Converting forests into rubber plantations weakened the soil CH 4 sink in tropical uplands. *Land Degrad. Dev.* **2019**, *30*, 2311–2322. [CrossRef]
21. Boisier, J.P.; De Nobletducoudre, N.; Pitman, A.; Cruz, F.T.; Delire, C.; Hurk, B.J.J.M.V.D.; van der Molen, M.; Müller, C.; Voldoire, A. Attributing the impacts of land-cover changes in temperate regions on surface temperature and heat fluxes to specific causes: Results from the first LUCID set of simulations. *J. Geophys. Res. Space Phys.* **2012**, *117*, 1–16. [CrossRef]
22. Houghton, R.A.; House, J.I.; Pongratz, J.; Van Der Werf, G.R.; DeFries, R.S.; Hansen, M.C.; Le Quéré, C.; Ramankutty, N. Carbon emissions from land use and land-cover change. *Biogeosciences* **2012**, *9*, 5125–5142. [CrossRef]
23. Pitman, A.J.; De Noblet-Ducoudré, N.; Cruz, F.T.; Davin, E.; Bonan, G.B.; Brovkin, V.; Claussen, M.; Delire, C.; Ganzeveld, L.; Gayler, V.; et al. Uncertainties in climate responses to past land cover change: First results from the LUCID intercomparison study. *Geophys. Res. Lett.* **2009**, *36*, 1–6. [CrossRef]
24. Bonan, G.B.; Levis, S.; Kergoat, L.; Oleson, K.W. Landscapes as patches of plant functional types: An integrating concept for climate and ecosystem models. *Glob. Biogeochem. Cycles* **2002**, *16*, 5-1–5-23. [CrossRef]
25. Fan, Y.; Meijide, A.; Lawrence, D.M.; Roupsard, O.; Carlson, K.M.; Chen, H.; Röll, A.; Niu, F.; Knohl, A. Reconciling Canopy Interception Parameterization and Rainfall Forcing Frequency in the Community Land Model for Simulating Evapotranspiration of Rainforests and Oil Palm Plantations in Indonesia. *J. Adv. Model. Earth Syst.* **2019**, *11*, 732–751. [CrossRef]
26. Post, H.; Hendricks Franssen, H.-J.; Han, X.; Baatz, R.; Montzka, C.; Schmidt, M.; Vereecken, H. Evaluation and uncertainty analysis of regional-scale CLM4.5 net carbon flux estimates. *Biogeosciences* **2018**, *15*, 187–208. [CrossRef]
27. Cheng, Y.; Huang, M.; Chen, M.; Guan, K.; Bernacchi, C.; Peng, B.; Tan, Z. Parameterizing Perennial Bioenergy Crops in Version 5 of the Community Land Model Based on Site-Level Observations in the Central Midwestern United States. *J. Adv. Model. Earth Syst.* **2020**, *12*, e2019MS001719. [CrossRef]
28. Fisher, R.A.; Wieder, W.R.; Sanderson, B.M.; Koven, C.D.; Oleson, K.W.; Xu, C.; Fisher, J.B.; Shi, M.; Walker, A.P.; Lawrence, D.M. Parametric Controls on Vegetation Responses to Biogeochemical Forcing in the CLM5. *J. Adv. Model. Earth Syst.* **2019**, *11*, 2879–2895. [CrossRef]

29. Lawrence, P.J.; Feddema, J.J.; Bonan, G.B.; Meehl, G.A.; O'Neill, B.C.; Oleson, K.W.; Levis, S.; Lawrence, D.; Kluzek, E.; Lindsay, K.; et al. Simulating the Biogeochemical and Biogeophysical Impacts of Transient Land Cover Change and Wood Harvest in the Community Climate System Model (CCSM4) from 1850 to 2100. *J. Clim.* **2012**, *25*, 3071–3095. [CrossRef]
30. Dahlin, K.M.; Fisher, R.A.; Lawrence, P.J. Environmental drivers of drought deciduous phenology in the Community Land Model. *Biogeosciences* **2015**, *12*, 5061–5074. [CrossRef]
31. Lawrence, D.M.; Fisher, R.A.; Koven, C.D.; Oleson, K.W.; Swenson, S.C.; Bonan, G.; Collier, N.; Ghimire, B.; van Kampenhout, L.; Kennedy, D.; et al. The Community Land Model Version 5: Description of New Features, Benchmarking, and Impact of Forcing Uncertainty. *J. Adv. Model. Earth Syst.* **2019**, *11*, 4245–4287. [CrossRef]
32. Chen, M.; Griffis, T.J.; Baker, J.M.; Wood, J.D.; Xiao, K. Simulating crop phenology in the Community Land Model and its impact on energy and carbon fluxes. *J. Geophys. Res. Biogeosci.* **2015**, *120*, 310–325. [CrossRef]
33. Wycherley, P.R. The Genus Hevea—Botanical Aspects. In *Natural Rubber*; Sethuraj, M.R., Mathew, N.M., Eds.; Developments in Crop Science; Elsevier: Amsterdam, The Netherlands, 1992; Volume 23, pp. 50–66. [CrossRef]
34. Kotowska, M.M.; Leuschner, C.; Triadiati, T.; Hertel, D. Conversion of tropical lowland forest reduces nutrient return through litterfall, and alters nutrient use efficiency and seasonality of net primary production. *Oecologia* **2016**, *180*, 601–618. [CrossRef] [PubMed]
35. Guardiola-Claramonte, M.; Troch, P.A.; Ziegler, A.D.; Giambelluca, T.W.; Vogler, J.B.; Nullet, M.A. Local hydrologic effects of introducing non-native vegetation in a tropical catchment. *Ecohydrology* **2008**, *1*, 13–22. [CrossRef]
36. Yeang, H.-Y. Synchronous flowering of the rubber tree (*Hevea brasiliensis*) induced by high solar radiation intensity. *New Phytol.* **2007**, *175*, 283–289. [CrossRef]
37. Zhai, D.-L.; Yu, H.; Chen, S.-C.; Ranjitkar, S.; Xu, J. Responses of rubber leaf phenology to climatic variations in Southwest China. *Int. J. Biometeorol.* **2019**, *63*, 607–616. [CrossRef]
38. Song, Q.-H.; Tan, Z.-H.; Zhang, Y.-P.; Sha, L.-Q.; Deng, X.-B.; Deng, Y.; Zhou, W.-J.; Zhao, J.; Zhang, X.; Zhao, W.; et al. Do the rubber plantations in tropical China act as large carbon sinks? *iForest-Biogeosci. For.* **2013**, *7*, 42–47. [CrossRef]
39. Bonan, G.B.; Lawrence, P.J.; Oleson, K.W.; Levis, S.; Jung, M.; Reichstein, M.; Lawrence, D.M.; Swenson, S.C. Improving canopy processes in the Community Land Model version 4 (CLM4) using global flux fields empirically inferred from FLUXNET data. *J. Geophys. Res. Biogeosci.* **2011**, *116*, 1–22. [CrossRef]
40. Margono, B.A.; Turubanova, S.; Zhuravleva, I.; Potapov, P.; Tyukavina, A.; Baccini, A.; Goetz, S.; Hansen, M.C. Mapping and monitoring deforestation and forest degradation in Sumatra (Indonesia) using Landsat time series data sets from 1990 to 2010. *Environ. Res. Lett.* **2012**, *7*, 034010. [CrossRef]
41. Ali, A.A.; Nugroho, B.; Moyano, F.E.; Brambach, F.; Jenkins, M.W.; Pangle, R.; Stiegler, C.; Blei, E.; Cahyo, A.N.; Olchev, A.; et al. Using a bottom-up approach to scale leaf photosynthetic traits of oil palm, rubber, and two coexisting tropical woody species. *Forests* **2021**, *12*, 359. [CrossRef]
42. Kotowska, M.M.; Leuschner, C.; Triadiati, T.; Meriem, S.; Hertel, D. Quantifying above- and belowground biomass carbon loss with forest conversion in tropical lowlands of Sumatra (Indonesia). *Glob. Chang. Biol.* **2015**, *21*, 3620–3634. [CrossRef] [PubMed]
43. Walker, A.P.; Hanson, P.J.; De Kauwe, M.G.; Medlyn, B.E.; Zaehle, S.; Asao, S.; Dietze, M.; Hickler, T.; Huntingford, C.; Iversen, C.M.; et al. Comprehensive ecosystem model-data synthesis using multiple data sets at two temperate forest free-air CO_2 enrichment experiments: Model performance at ambient CO_2 concentration. *J. Geophys. Res. Biogeosci.* **2014**, *119*, 937–964. [CrossRef]
44. Fan, Y.; Roupsard, O.; Bernoux, M.; Le Maire, G.; Panferov, O.; Kotowska, M.M.; Knohl, A. A sub-canopy structure for simulating oil palm in the Community Land Model (CLM-Palm): Phenology, allocation and yield. *Geosci. Model Dev.* **2015**, *8*, 3785–3800. [CrossRef]
45. Koven, C.D.; Riley, W.J.; Subin, Z.M.; Tang, J.Y.; Torn, M.S.; Collins, W.D.; Bonan, G.B.; Lawrence, D.M.; Swenson, S.C. The effect of vertically resolved soil biogeochemistry and alternate soil C and N models on C dynamics of CLM4. *Biogeosciences* **2013**, *10*, 7109–7131. [CrossRef]
46. Viovy, N. *CRUNCEP Version 7—Atmospheric Forcing Data for the Community Land Model*; National Center for Atmospheric Research, Computational and Information Systems Laboratory: Boulder, CO, USA, 2018. [CrossRef]
47. Meijide, A.; Badu, C.S.; Moyano, F.; Tiralla, N.; Gunawan, D.; Knohl, A. Impact of forest conversion to oil palm and rubber plantations on microclimate and the role of the 2015 ENSO event. *Agric. For. Meteorol.* **2018**, *252*, 208–219. [CrossRef]
48. Li, Y.; Lan, G.; Xia, Y. Rubber Trees Demonstrate a Clear Retranslocation Under Seasonal Drought and Cold Stresses. *Front. Plant Sci.* **2016**, *7*, 1907. [CrossRef]
49. Waite, P.-A. Variability of Wood and Leaffunctional Traits in Response to Structural and Environmental Changes in Natural and Transformed Systems in Indonesia. Ph.D. Thesis, University of Goettingen, Goettingen, Germany, June 2020.
50. Priyadarshan, P.M. *Biology of Hevea Rubber*; CAB International: Wallingford, UK, 2011.
51. Carr, M.K.V. The water relations of rubber (*Hevea Brasiliensis*): A review. *Exp. Agric.* **2012**, *48*, 176–193. [CrossRef]
52. Perron, T.; Mareschal, L.; Laclau, J.-P.; Deffontaines, L.; Deleporte, P.; Masson, A.; Cauchy, T.; Gay, F. Dynamics of biomass and nutrient accumulation in rubber (*Hevea brasiliensis*) plantations established on two soil types: Implications for nutrient management over the immature phase. *Ind. Crop. Prod.* **2020**, *159*, 113084. [CrossRef]
53. Chairungsee, N.; Gay, F.; Thaler, P.; Kasemsap, P.; Thanisawanyangura, S.; Chantuma, A.; Jourdan, C. Impact of tapping and soil water status on fine root dynamics in a rubber tree plantation in Thailand. *Front. Plant Sci.* **2013**, *4*, 538. [CrossRef]

54. Zhou, R.; Zhang, Y.; Song, Q.; Lin, Y.; Sha, L.; Jin, Y.; Liu, Y.; Fei, X.; Gao, J.; He, Y.; et al. Relationship between gross primary production and canopy colour indices from digital camera images in a rubber (*Hevea brasiliensis*) plantation, Southwest China. *For. Ecol. Manag.* **2019**, *437*, 222–231. [CrossRef]
55. Cahyo, A.N.; Ardika, R.; Wijaya, T. Water consumption and rubber production on various planting space arrangement system and their relationship with soil water content. *Indones. J. Nat. Rubber Res.* **2011**, *29*, 110–117.
56. Oktavia, F.; Lasminingsih, M. Effect of rubber plant leaves development to production variation in IRR series clones. *Indones. J. Nat. Rubber Res.* **2010**, *28*, 32–40.
57. Chantuma, P.; Lacointe, A.; Kasemsap, P.; Thanisawanyangkura, S.; Gohet, E.; Clement, A.; Guilliot, A.; Ameglio, T.; Thaler, P. Carbohydrate storage in wood and bark of rubber trees submitted to different level of C demand induced by latex tapping. *Tree Physiol.* **2009**, *29*, 1021–1031. [CrossRef] [PubMed]
58. Silpi, U.; Lacointe, A.; Kasempsap, P.; Thanysawanyangkura, S.; Chantuma, P.; Gohet, E.; Musigamart, N.; Clement, A.; Ameglio, T.; Thaler, P. Carbohydrate reserves as a competing sink: Evidence from tapping rubber trees. *Tree Physiol.* **2007**, *27*, 881–889. [CrossRef]
59. Barman, R.; Jain, A.K.; Liang, M. Climate-driven uncertainties in modeling terrestrial gross primary production: A site level to global-scale analysis. *Glob. Chang. Biol.* **2014**, *20*, 1394–1411. [CrossRef]
60. Ali, A.A.; Xu, C.; Rogers, A.; Fisher, R.A.; Wullschleger, S.D.; Massoud, E.C.; Vrugt, J.A.; Muss, J.D.; McDowell, N.G.; Fisher, J.B.; et al. A global scale mechanistic model of photosynthetic capacity (LUNA V1.0). *Geosci. Model Dev.* **2016**, *9*, 587–606. [CrossRef]
61. Whitley, R.J.; Macinnis-Ng, C.M.O.; Hutley, L.; Beringer, J.; Zeppel, M.; Williams, M.; Taylor, D.; Eamus, D. Is productivity of mesic savannas light limited or water limited? Results of a simulation study. *Glob. Chang. Biol.* **2011**, *17*, 3130–3149. [CrossRef]
62. Schaefer, K.; Schwalm, C.; Williams, C.A.; Arain, M.A.; Barr, A.; Chen, J.M.; Davis, K.J.; Dimitrov, D.; Hilton, T.; Hollinger, D.Y.; et al. A model-data comparison of gross primary productivity: Results from the North American Carbon Program site synthesis. *J. Geophys. Res. Space Phys.* **2012**, *117*, 1–15. [CrossRef]
63. Ankomah, G.O. Assessment of Leaf Area Index and Canopy Openness Across Four Land-Use Systems in Jambi Province, Sumatra, Indonesia. Master's Thesis, University of Goettingen, Goettingen, Germany, March 2019.
64. Niu, F.; Röll, A.; Meijide, A.; Hendrayanto; Hölscher, D. Rubber tree transpiration in the lowlands of Sumatra. *Ecohydrology* **2017**, *10*, e1882. [CrossRef]
65. Hassler, E.; Corre, M.D.; Tjoa, A.; Damris, M.; Utami, S.R.; Veldkamp, E. Soil fertility controls soil–atmosphere carbon dioxide and methane fluxes in a tropical landscape converted from lowland forest to rubber and oil palm plantations. *Biogeosciences* **2015**, *12*, 5831–5852. [CrossRef]
66. Igarashi, Y.; Katul, G.; Kumagai, T.; Yoshifuji, N.; Sato, T.; Tanaka, N.; Tanaka, K.; Fujinami, H.; Suzuki, M.; Tantasirin, C. Separating physical and biological controls on long-term evapotranspiration fluctuations in a tropical deciduous forest subjected to monsoonal rainfall. *J. Geophys. Res. Biogeosci.* **2015**, *120*, 1262–1278. [CrossRef]
67. Dawoe, E.K.; Isaac, M.E.; Quashie-Sam, J. Litterfall and litter nutrient dynamics under cocoa ecosystems in lowland humid Ghana. *Plant Soil* **2010**, *330*, 55–64. [CrossRef]
68. Hirata, R.; Saigusa, N.; Yamamoto, S.; Ohtani, Y.; Ide, R.; Asanuma, J.; Gamo, M.; Hirano, T.; Kondo, H.; Kosugi, Y.; et al. Spatial distribution of carbon balance in forest ecosystems across East Asia. *Agric. For. Meteorol.* **2008**, *148*, 761–775. [CrossRef]
69. Ali, A.A.; Fan, Y.; Corre, M.D.; Kotowska, M.M.; Hassler, E.; Cahyo, A.N.; Moyano, F.E.; Stiegler, C.; Röll, A.; Meijide, A.; et al. Data and Codes for a Rubber Plant Functional Type in the Community Land Model (CLM5). 2021. Available online: https://zenodo.org/record/4729044#.Ye5Mr6ERV9A (accessed on 30 April 2021).
70. Oleson, K.; Lawrence, D.; Bonan, G.; Drewniak, B.; Huang, M.; Koven, C.; Levis, S.; Li, F.; Riley, W.; Subin, Z.; et al. *Technical Description of Version 4.5 of the Community Land Model (CLM)*; National Center for Atmospheric Research: Boulder, CO, USA, 2013. [CrossRef]